NJC

Accepted Manuscript

Volume 40 | Number 1 | January 2016 | Pages 1–846

NJC

New Journal of Chemistry
www.rsc.org/njc

A journal for new directions in chemistry

ISSN 1144-0546

ROYAL SOCIETY
OF CHEMISTRY

PAPER
Jason B. Benedict et al
The role of atropisomers on the photo-reactivity and fatigue of
diarylethene-based metal–organic frameworks

CNRS

ROYAL SOCIETY
OF CHEMISTRY

rsc.li/njc

ROYAL SOCIETY OF CHEMISTRY

Journal Name

ARTICLE

Heterogenized chiral iminoindanol complex of manganese as an efficient catalyst for aerobic epoxidation of olefins

Vahideh Abbasi, Hassan Hosseini-Monfared[*] and Seyed Majid Hosseini

A new heterogenized chiral catalyst, GFC-[Mn(L)(OH)], was synthesized by grafting complex [Mn(L)(OH)] on carbon coated magnetic Fe_3O_4 nanoparticles decorated reduced graphene oxide sheets (GFC) through the amine linkage (L = (1R,2S)-1-(N-salicylideneamino)-2-indanol). The catalyst was characterized by FT-IR, UV/Vis, XRD, SEM and vibrating sample magnetometer (VSM) techniques. It exhibited excellent activity and selectivity in the epoxidation of olefins with oxygen in the presence of isobutyraldehyde under mild conditions (conversion 38-98%; selectivity 65- 98%; enantioselectivity 58-100, except alpha-methylstyrene). Furthermore, synergistic effect of reduced graphene oxide support was observed on the increasing activity, epoxide selectivity and enantioselectivity. The catalyst could be recovered by magnetic separation from the reaction mixture and recycled five times without any significant loss in its activity. The advantage of this development is using both the synergic effect of reduced graphene oxide and magnetite nanoparticles to obtain an easily recyclable heterogeneous green catalyst. In addition, the high asymmetry induction of rigid indanol-based unit of the ligand results to high enantioselectivity.

Introduction

Chiral epoxides are useful starting reagent for the synthesis of various desirable chiral products by stereospecific ring-opening reactions.[1] Chiral compounds are commonly required in pharma, agrochemical and fine chemical sectors. In addition, to prevent a tragedy such as thalidomide drug, pharmaceutical companies nowadays have to make sure that both enantiomers of a drug are tested for their biological activity and toxicity before they are marketed. Obviously, there is a strong demand for the pure enantiomers.

Before the advent of enantioselective reactions, chiral compounds had to be biosynthetically made or resolved. This was an expensive and time consuming process, especially for industrial applications. Catalytic oxidation of olefins is an economically favourite protocol to get chiral epoxides.[2,3,4,5] Further improvement is to use a heterogeous catalyst. There are several reasons to consider a heterogenization method for using chiral metal complexes as catalyst. First the price of the chiral ligands and complexes are usually high. Second obtaining pure products without residual catalysts or residual catalyst ligands, and finally due to the environmental problem which is associated with catalyst/ligand waste or associated with the processes of their separation from a product.[6] Most

of these justifications for enantioselective catalyst and ligand recovery are examples of the trend towards 'green chemistry' processes.[7] A single atom sheet graphene with carbon atoms in a sp^2 hexagonal bonding configuration possesses high thermal conductivity and high surface area of 2630 m^2/g [8] which make it a superior candidate to use as support for heterogenization of catalysts. Metal-organic ligand complexes can be linked covalently to oxygen-containing functional groups of graphene oxide (GO) and in addition to heterogenization benefit from the enhanced activity by the synergic interactions between the complex and GO.[9] Additionally, the existence of anchored complexes will prevent the aggregation of GO sheets during the reduction, and keep the specific surface area of the resultant hybrid materials large, which is required for catalysis.[10] Lately Zheng et al loaded L-proline onto GO and used in asymmetric aldol reaction.[11] Nasseri et al reported the use of a Mn(III) complex supported on GO for the epoxidation of olefins using *m*-CPBA as an oxidant.[12]

To overcome to the problem of GO-metal complex separation from a reaction medium a fast and clean method is to use magnetic nanoparticles. GO-metal complex can be decorated with magnetic nanoparticles and then easily separated by magnetic decantation.[13] Decorating graphene sheets with Fe_3O_4 nanoparticles (NPs) will impart desirable magnetic properties to the graphene, making the composites promising for a variety of applications in fields such as catalysis and environmental remediation.[14] Coating Fe_3O_4 NPs with carbonaceous shells protect them from being dissolved in

Department of Chemistry, University of Zanjan, 45195-313 Zanjan, Iran.
E-mail: monfared@znu.ac.ir (H. Hosseini-Monfared); Tel.: +98 24 33052576; Fax: +98 24 33583203.

New Journal of Chemistry Accepted Manuscript

ARTICLE   **Journal Name**

acidic or basic media and Fe_3O_4@C have exhibited high stability at high temperature and pressure. Magnetic graphene–Fe_3O_4@carbon (GFC) has been used successfully for dye adsorption.[10]

Chiral manganese(III) salen complexes show enantioselective catalytic activity in the epoxidation of olefins.[15] Salicylidene Schiff base derivatives also form stable transition metal complexes for polymerization,[16] enantioselective and selective epoxidation of olefins.[17,18,19,20,21] *Cis*-aminoindanol as a chiral amino alcohol is a good chiral motif which can be used for the preparation of a chiral Schiff base. The availability of optically active cis-1-amino-2-indanol and the high levels of asymmetry it induces are useful for the development of economical large-scale processes. *Cis*-1-amino-2-indanol-based chiral auxiliaries have been used for carbon-carbon and carbon-heteroatom bond formations reactions.[22] The rigidity of indane increases the asymmetric transmission during the catalysis. Condensation of chiral *cis*-1-amino-2-indanol with salicylaldehyde results to a non-C_2-symmetric Schiff base ligand.

In continuation of our ongoing research on the application of heterogeneous catalysts in organic synthesis and development of novel catalytic oxidation methods using environmentally benign oxidants such as O_2,[23,24] we now report the design and application of the covalent attachment of [Mn(L)(OH)] (L = (1S,2R)-1-(N-salicylideneamino)-2-indanol) onto carbon coated magnetic Fe_3O_4 nanoparticles supported on reduced graphene oxide sheets (GFC). It was proved that the new catalyst GFC-[Mn(L)(OH)] is efficient for the enantioselective epoxidation of unfunctionalized olefins with O_2 in combination with a sacrificial coreductant isobutyraldehyde. GFC-[Mn(L)(OH)] was recovered from the reaction mixture by using an external magnetic field.

Experimental

(1*R*,2*S*)-(+)-*cis*-1-amino-2-indanol and all other reagents with high purity were purchased from Fluka and used as received. IR spectra were taken with a Matson FT-IR spectrophotomer in the range of 400–4000 cm^{-1} as KBr disks. UV/Vis spectra of solutions were recorded with a Shimadzu 160 spectrophotometer. The UV/Vis spectra of the solid nanostructures were evaluated in the range of 190-800 nm by using spectrophotometer Shimadzu-UV-2550-8030 with slit width of 5.0 nm and light source with wavelength of 360.0 nm at room temperature. Powder X-ray diffraction (XRD) data were recorded on a Bruker D8 ADVANCED diffractometer with Cu Kα radiation (λ = 1.5418 Å). The surface morphologies of the nanocomposites were identified by the scanning electron microscope Stereo scan 360 (leica/Cambridge) and Hitachi f4160. The Mn content of the catalysts was determined by Varian AA-220 Atomic absorption spectroscopy (AAS). A HP Aglient 6890 gas chromatograph which was equipped by a HP-5 capillary column (phenyl methyl siloxane 30 mm×320 μm×0.25 μm) and flame-ionization detector was used quantification of the oxidation reaction products. The enantiomeric excess (ee%) was determined by chiral GC (HP

6890-GC) using a SGE-CYDEX-B capillary column (25 m × 0.22 mm × 0.25 μm). The configuration (*R* or *S*) of the chiral products was assigned by comparison of retention times with those of R-(+)-limonene. ^{1}H NMR spectra were recorded on a Bruker 250 MHz spectrometer.

The reduced graphene oxide/Fe_3O_4 hybrid (rGO/Fe_3O_4) and its functionalization with the amine rGO/Fe_3O_4@C-NH_2 (GFC-NH_2) was synthesized according to our previous report.[25]

Synthesis of (1*R*,2*S*)-1-(N-salicylideneamino)-2-indanol (H₂L)

The mixture of (1*R*,2*S*)-(+)-*cis*-1-amino-2-indanol (0.50 g, 3.35 mmol), 2-hydroxybenzaldehyde (0.78 g, 3.35 mmol) and anhydrous Na_2SO_4 (2.00 g) in dry methanol (25 mL) was refluxed for 4 h. The yellow solid was separated by filtration and recrystallized from dry methanol. Yield 70% (0.70 g). IR (KBr) 3418, 3131, 1638, 744 cm^{-1}. ^{1}H NMR (250.13 MHz, $CDCl_3$): δ = 12.94 (s, 1H,vb), 8.62 (s, 1H), 7.39-7.16 (m, 6H), 6.99-6.91 (m, 2H), 4.82 (d, 1H, J = 6 Hz), 4.70 (dd, 1H, J = 6 Hz, J = 11 Hz), 3.27 (dd, 1H, J = 6 Hz, J = 16 Hz), 3.11 (dd, 1H, J = 5 Hz, J = 16 Hz), 2.16 (s, 2H, vb) ppm. ^{13}C NMR (62.90 MHz, $CDCl_3$): δ = 167, 161, 141, 133, 132, 129, 127, 126, 125, 119, 117, 76, 75, 40 ppm.

Synthesis of [Mn(L)(OH)]

Following a reported procedure for the synthesis of Schiff bases,[20] $MnCl_2 \cdot 4H_2O$ (1.09 g, 5.4 mmol) was added to the solution of H₂L (0.70 g, 2.7 mmol) in dry methanol (15 ml) and gently refluxed for 8 h. The solvent was evaporated and the resulting black solid washed two times with water. The product was dried overnight at room temperature. Yield 74% (0.69 g). Anal. Calcd for $C_{16}H_{14}MnNO_3$: C, 59.45; H, 4.37; N, 4.33. Found: C, 58.94; H, 4.48; N, 4.00. IR (KBr): v̄ = 3423 (m, O-H), 3020 (w), 2923 (m), 2853 (w), 1612 (vs, C=N), 1127 (m), 1092 (s), 1306 (s), 1045 (s), 754 (vs), 462 (w) cm^{-1}.

Synthesis of nanocomposite GFC-[Mn(L)(OH)]

A certain amount of [Mn(L)(OH)] (0.54 g) was added to GFC-NH_2 (0.7 g) in methanol and refluxed under a nitrogen atmosphere for 24 h. The resulting product was isolated by magnetic separation, washed with large quantities of methanol and water.

As a control experiment, Fe_3O_4@C[Mn(L)(OH)] was prepared using a reported procedure[25] under the same conditions without using graphene oxide

Catalytic tests

The oxidation of olefins with O_2 was performed in a 25-mL round-bottom flask equipped with a refluxing condenser and a small magnetic bar. In a typical experiment the flask was charged with the suspension of catalyst (10.0 mg containing 0.66 μmol Mn), acetonitrile (3 mL), substrate (2 mmol) and isobutyraldehyde as oxygen acceptor (5 mmol). Dioxygen, as oxidant, was filled in the system by using an oxygen balloon. The flask was placed in a thermostatic oil bath at 25, 40 or 60 °C. Reactions were carried out for 8 h under vigorous magnetic

stirring. At appropriate intervals, aliquots were removed and analyzed by GC using a HP-5 capillary column (phenyl methyl siloxane 30 mm×320 μm×0.25 μm) and a chiral SGE-CYDEX-B capillary column (25 m × 0.22 mm × 0.25 μm). The reaction products were quantified by gas chromatography using calibration curve. The reported results are the average of three repeated experiments. The products were identified with authentic samples and/or ^{1}H-NMR spectroscopic data.

Control reactions were carried out in the absence of catalyst, under the same conditions as the catalytic runs. The recyclability of GFC-[Mn(L)(OH)] catalyst was carried out by separating the catalyst from the reaction system by magnetic decantation. It was washed with methanol and acetonitrile and dried at 60 °C, then reused in the next reaction.

Results and discussion

Synthesis and characterization of GFC-[Mn(L)(OH)]

Graphite powder was oxidized using a modified Hummers' procedure to produce graphene oxide. FT-IR spectra of the synthesized graphene oxide (GO) and graphite are shown in Fig. S1 (in Electronic Supplementary Information, ESI). The FT-IR spectrum of GO shows an O–H bond as a broad peak at 3422 cm^{-1}. In GO the presence of C=O, C=C, C–OH and C–O (epoxy) functional groups were appeared as strong bands at 1720, 1619, 1223 and 1054 cm^{-1}, respectively.[8] The spectrum of GO also shows a C=C peak at 1583 cm^{-1} and a C-O peak at 1054 cm^{-1} corresponding to the remaining sp^2 character and alkoxy group, respectively. Graphite and GO were grossly similar, whereas the characteristic peaks in the spectrum of GO do not appear in the curve of graphite.

Black coloured chiral ligand H$_2$L was prepared in good yield by condensation of salicylaldehyde and chiral (1*R*,2*S*)-(+)-*cis*-1-amino-2-indanol in refluxing methanol. Also complex [Mn(L)(OH)] was synthesized in methanol under reflux condition in a very good yield (74%) and purity by treatment of H$_2$L with MnCl$_2$. Reduced GO was organofunctionaized by the condensation reaction of 3-(aminopropyl)trimethoxysilane and the GFC active C-OH groups to produce GFC-NH$_2$. Complex [Mn(L)(OH)] was sequentially immobilized onto the support by coordination with the NH$_2$ of GFC-NH$_2$ as illustrated in Scheme 1. The main spectroscopic feature of H$_2$L is as follows. In the infrared spectrum (Fig. 1), an absorption band at 1639 cm^{-1} shows the characteristic of the imine C=N stretching and broad bands at 3423 and 3166 cm^{-1} are due to the phenolic and the aminoindanol unit proton hydrogen bonded to the imine

nitrogen (O–H···N). In general, hydrogen bonding[26] to an X-H molecule results in a decrease in the frequency and a broadening of the absorption band that is assigned to the O-H stretching vibration. The infrared analysis of the resulting manganese complex revealed the weakening of the band at 3423 cm^{-1} and the disappearance of the broad band about 3166 cm^{-1} in the free ligand indicating deprotonation of the ligand and replacement by the metal ion. A shift to lower frequency 1612 cm^{-1} of the band for the imine group is observed upon metal coordination relative to the free ligand 1639 cm^{-1}, indicating participation of the nitrogen atom in metal complexation.[27] The IR spectrum of GFC-[Mn(L)(OH)] shows (Fig. 1) new weak peaks in the range of 1600–1100 cm^{-1} owing to C-O, C-N and aromatic ring vibrations which confirm the successful immobilization of the complex onto GFC.

The UV/Vis spectrum of GO shows a strong absorption peak at 231 nm and a shoulder at about 305 nm, which are attributed to the $\pi \rightarrow \pi^*$ transition of graphitic C–C bonds and to the $n \rightarrow \pi^*$ transitions of C=O bonds, respectively.[8] After reduction, the rGO/Fe$_3$O$_4$ absorption peak red shifted to 248 nm because the electronic conjugation in the graphene was restored by the reduction with sodium acetate.[28] The UV/Vis spectrum of ligand H$_2$L shows two absorption bands (λ_{max} = 260 and 323 nm) and the corresponding Mn-L complex shows intense UV absorption bands (λ_{max} = 261 and 328 nm) and a weak visible absorption band at 400 nm. The UV bands for both the ligand and complex have been assigned to ligand-centred π-π^* transitions (Fig. 2) and the visible absorption band of Mn-L has been assigned to the hydroxyl and phenolate O (p$_\pi$) $\rightarrow$ Mn(d$_{\pi*}$) ligand to metal charge-transfer (LMCT) transitions.[29] Elemental analyses and chloride titration measurements confirmed the absence of chloride ligand.The tridentate H$_2$L ligand of the complex adopts a near-planar geometry around the Mn(III) ion and therefore the complex containing the hydroxide ion as the fourth ligand approaches the structure of a distorted square planar. However, such a complex easily passes at six coordination of the pseudo-octahedral type by forming adducts with electron donating atoms from surroundings (e.g. donor atoms of the solvent). It is known that the complexes of Mn(III) ion in an octahedral environment should give rise to spin allowed absorption peaks as well as to spin forbidden ones due to its d^4 electronic structure;[30] these should exhibit a broad strong band at 476-625 nm. Complex [Mn(L)(OH)] does not show absorption in the visible region, presumably because the weak d–d bands are submerged in the tail of the charge transfer bands.

Journal Name

ARTICLE
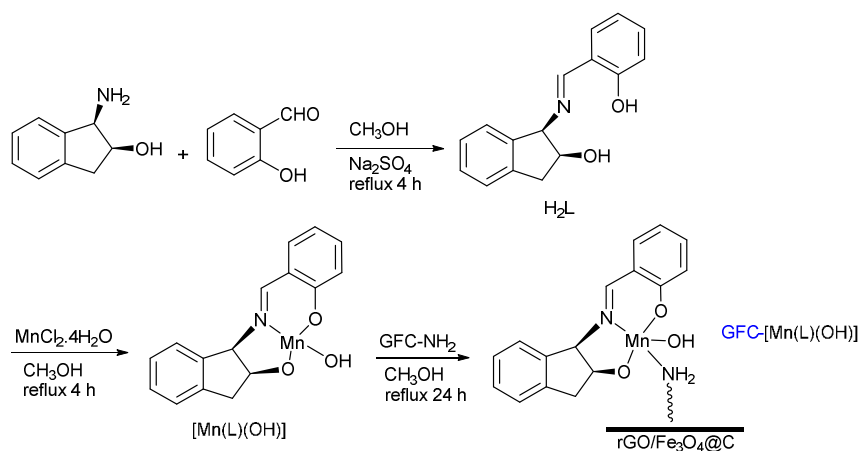
Scheme 1 The syntheses of H_2L, chiral complex [Mn(L)(HO)] and its immobilization on GFC.
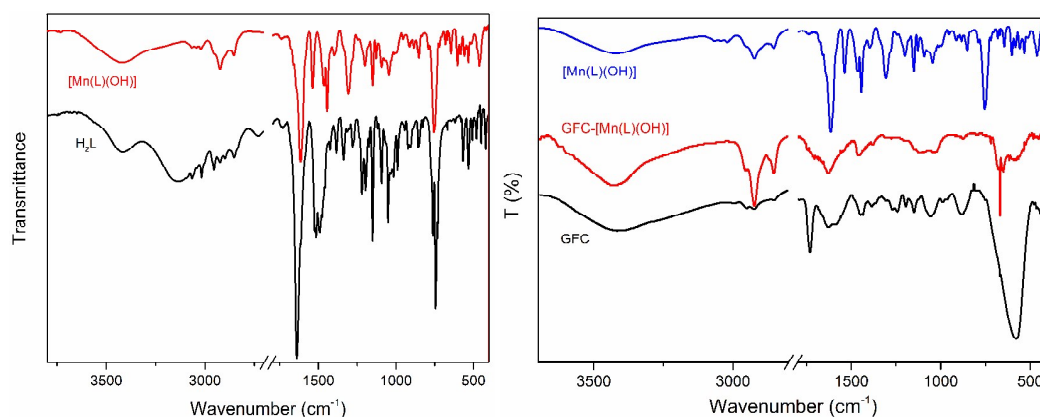
Fig. 1 FT-IR spectra of chiral H_2L, [Mn(L)(OH)] (left) and GFC, complex, GFC-complex (right).

The composite of reduced graphene oxide/Fe_3O_4@C containing [Mn(L)(OH)] complex is black-brown in colour, this colour arising from the strong absorption band of the complex at low wavelength (< 350 nm) tailing to beyond 400 nm as shown in Fig. 2 for a solution in ethanol. Diffuse reflectance spectrum of the investigated composite is also presented in Fig. 2. The main π-π* peaks shifted toward the higher energies; the ligand to metal charge transfer (CT) peak at 400 nm shifted toward the lower energy. These shifts could be consistent with the complex distortion onto the GFC; in this case, the spectrum is an evidence for immobilization of the complex on the support.
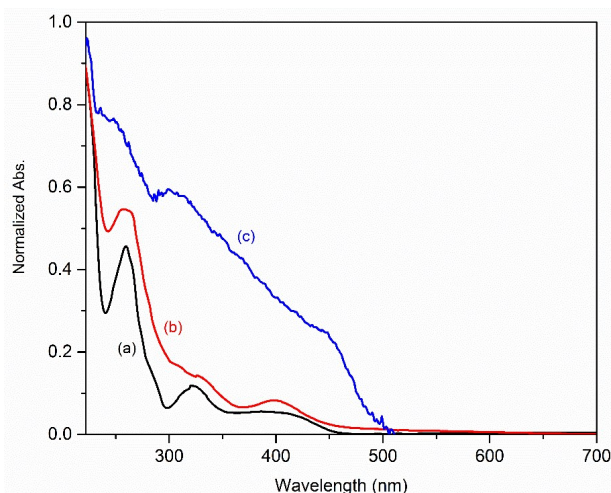
Journal Name   **ARTICLE**

Fig. 2 UV/Vis spectra of (a) H_2L and (b) [Mn(L)(OH)] recorded in ethanol solution and (c) DR-UV of GFC-[Mn(L)(OH)].

Fig. 3 XRD patterns of graphite, GO, rGO/Fe$_3$O$_4$, GFC and composite [GFC-[Mn(L)(OH)].

XRD analysis

The XRD patterns of graphite, GO, rGO/Fe$_3$O$_4$, GFC and composite GFC-[Mn(L)(OH)] are shown in Fig. 3. Graphite powder exhibits a high crystalline degree with a strong and sharp diffraction peak at $2\theta = 26.37°$. In contrast, the crystalline degree of graphite oxide is very low due to a preserved graphene like honeycomb lattice in graphite oxide. The oxidation of graphite led to the shift of the diffraction peak position from $2\theta = 26.6$ to $12.1–11.2$ Å, corresponding to the increase in the inter planar distance because of the attachment of oxygen functional groups to both sides of the single graphene layer during its oxidation.[31] The diffraction pattern of the GFC shows that the carbon shell prepared by this method is amorphous; a similar trace to the graphene–Fe$_3$O$_4$ hybrid but no obvious sharp diffraction peak for the graphite is observed, confirming that.[10] In Fig. 3 by immobilization of the homogeneous [Mn(L)(OH)] complex on graphene oxide, 002 reflections peak of GO was completely disappeared and structure of Fe$_3$O$_4$@C are not destroyed during immobilization of the complexes. The crystallite size of 14.1 nm was calculated for GFC-[Mn(L)(OH)] using the X'Pert program.

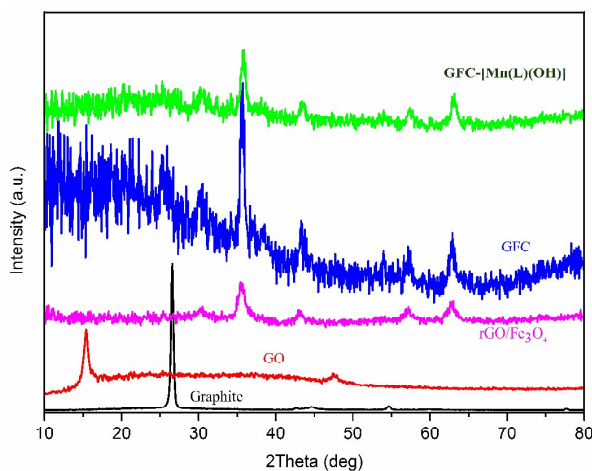## Magnetization studies

Magnetization studies showed that Fe$_3$O$_4$ and GFC-[Mn(L)(OH)] hybrid are superparamagnetic (Fig. 4) since there were no hysteresis in the magnetization curves at room temperature with an applied magnetic field sweeping from -10000 to +10000 k$_{Oe}$.[Error! Bookmark not defined.] The specific saturation magnetization (Ms) is 58.3 emu g^{-1} for Fe$_3$O$_4$ and 11 emu g^{-1} for the GFC-[Mn(L)(OH)] hybrid. For composite GFC-[Mn(L)(OH)], the decrease in the value of Ms could be attributed to the reduced amount of Fe$_3$O$_4$. The magnetization value of GFC-[Mn(L)(OH)] is comparable with previous reports[32] and is strong enough to be easily separated using a magnet.

SEM analysis

The thick cakes of graphite seen in the SEM measurement (Fig. 5a) have been exfoliated into thin large flakes of GO (Fig. 5b) after oxidation. Graphite shows its flat surface with many small and dispersed flakes and an ordered layer structure. The primary graphite structure disrupted into crumpled layer structure due to its oxidation. Nanoparticles of Fe$_3$O$_4$@C in GFC are seen as large number of granular particles closely attach on the surface of rGO sheets (Fig. 5c), indicating the formation of loosely packed Fe$_3$O$_4$ nanoparticles onto rGO sheets. The image of the GFC-[Mn(L)(OH)] represented in Fig. 5d, clearly shows that the nanoparticle was immobilized onto the GFC surface. Graphene sheets dispersed Fe$_3$O$_4$ nanoparticles and prevent their self-aggregation.
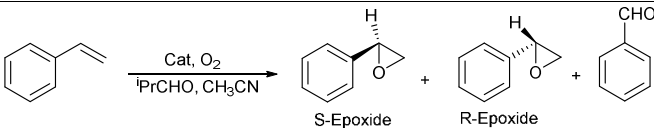
ARTICLE

Journal Name
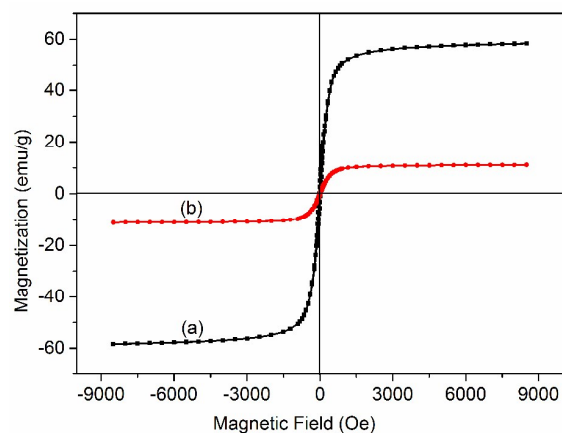
Fig. 4 Magnetization curves of (a) Fe_3O_4 and (b) GFC-[Mn(L)(OH)].
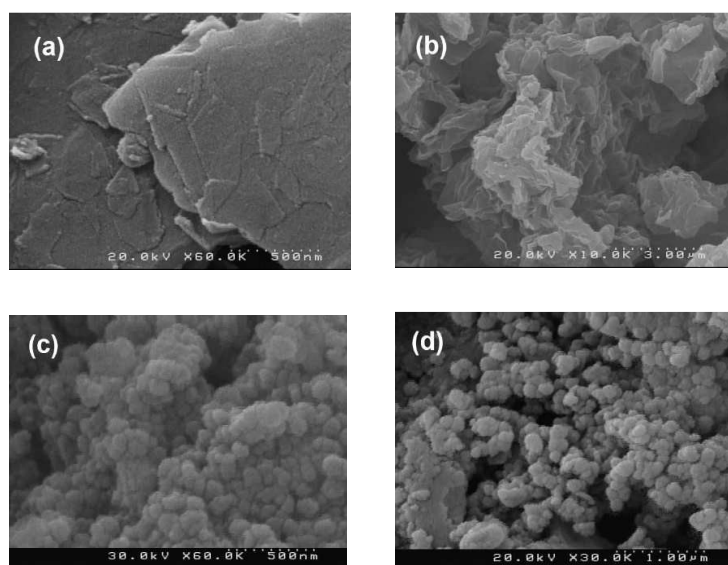
Fig. 5 SEM images of (a) graphite, (b) GO, (c) rGO/Fe_3O_4 and (d) GFC-[Mn(L)(OH)]

Catalytic activity

The catalytic activity of [Mn(L)(OH)] in solution (homogeneous catalysis) and in heterogenized form as GFC-[Mn(L)(OH)] were investigated in the oxidation of styrene using O_2 as oxidant. Results are presented in Table 1. Control experiments revealed that the reaction is catalytic (Table 1, entry 1) and

isobutyraldehyde as co-catalyst (entry 2) are essential for the oxidation. Replacing O_2 by air decreased the conversion (entry 3).

Co-oxidation of styrene and isobutyraldehyde under the investigated conditions leads to the formation of styrene oxide/benzaldehyde (main products). Isobutyraldehyde was co-oxidized with styrene to isobutyric acid. Comparison of

Journal Name

ARTICLE

Table 1 Catalytic oxidation of styrene.[a]

Entry	Time (h)	Catalyst/cocatalyst/oxidant	Conv. (%)[b]	Epoxide selectivity (%)[b]	Ee (%) (conf.)[c]
1	8	None/^{i}PrCHO/O$_2$	< 3	0	0
2	8	GFC-[Mn(L)(OH)]/none/O$_2$	0	0	0
3	8	GFC-[Mn(L)(OH)]/^{i}PrCHO/air	37	84	74 (S)
4	8	FC-[Mn(L)]/^{i}PrCHO/O$_2$	54	37	40 (S)
5	**2**	**GFC-[Mn(L)(OH)]/^{i}PrCHO/O$_2$**	**100**	**78**	**67 (S)**
6	2	[Mn(L)(OH)]/^{i}PrCHO/O$_2$	83	54	73 (S)
7	4	[Mn(L)(OH)]/^{i}PrCHO/O$_2$	100	60	57 (S)

[a] Reaction conditions: catalyst 10 mg (containing 0.66 μmol Mn), styrene 2 mmol, O$_2$ 1 bar, CH$_3$CN 3 mL, ^{i}PrCHO 5 mmol and temperature 40° C. Reported results are the average of at least two experiments. [b] Conversion and selectivity were determined by GC. [c] The enantiomeric excess (ee) values were determined by GC analysis on a chiral stationary phase (see the Experimental section).

Fe$_3$O$_4$@C (shown as FC in Table 1) and GFC as catalyst supports revealed the favourable synergic effect of the reduced graphene oxide (entries 4 and 5). Epoxide selectivity of GFC-[Mn(L)(OH)] was higher than that of homogeneous [Mn(L)(OH)] (entry 6). Furthermore, although the oxidation of styrene with GFC-[Mn(L)(OH)]/^{i}PrCHO/O$_2$ system was quantitative within 2 h, it proceeded up to 83% by the homogeneous [Mn(L)(OH)]/^{i}PrCHO/O$_2$ system. Increasing the reaction time up to 4 h increased the conversion, but decreased ee from 73% to 57% (entry 7).

The superior reactivity of GFC-[Mn(L)(OH)] in the aerobic oxidation of styrene is attributed to the promotion role of graphene support in the adsorption of reactant styrene and oxygen in addition to the site isolation of active species.[9] Assuming site isolation effect by immobilization,[33,34] the manganese catalytic sites can be separated from each other and keep the high efficiency throughout the whole catalytic process. Synergistic catalyst–support interactions has also been reported in a graphene–Mn$_3$O$_4$ electrocatalyst for vanadium redox flow batteries.[35] What is more, reduced graphene oxide probably is involved in epoxide selectivity by increasing the electron cloud density around the complex Mn-centre. These characters further make for the smooth proceeding and excellent selectivity of the conversion process. In the meantime, the covalent linkage of the Mn-L to rGO and chelate structure of the ligand ensures the robust immobilization of manganese complex onto the rGO surface, which accounts for the remarkable reusability and stability of the immobilized catalyst.

The choice of solvent is crucial in the epoxidation of olefins. The oxidation of styrene performed in different solvents, namely acetonitrile, ethyl acetate, methanol and *n*-hexane

(Fig. 6). The best conversion, epoxide selectivity and enantioselectivity were obtained in acetonitrile with relative dielectric constant ε/ε° = 37.5. Although the oxidation in ethyl acetate was high (conversion 92%), very low epoxide selectivity was observed (selectivity 13%). The catalytic activity of catalyst GFC-[Mn(salan)Cl] decreased in order acetonitrile > ethyl acetate > *n*-hexane > methanol =THF.

Effect of the reaction temperature on the catalytic activity of GFC-[Mn(L)Cl/O$_2$/^{i}PrCHO system was also remarkable. The catalyst activity increased by increasing the reaction temperature from 0 to 40 °C (Fig. 7). The catalyst showed maximum activity at 40 °C and conversion of 100% was obtained after 2 h. These findings propose the formation of active intermediate at temperature higher than 0 °C.
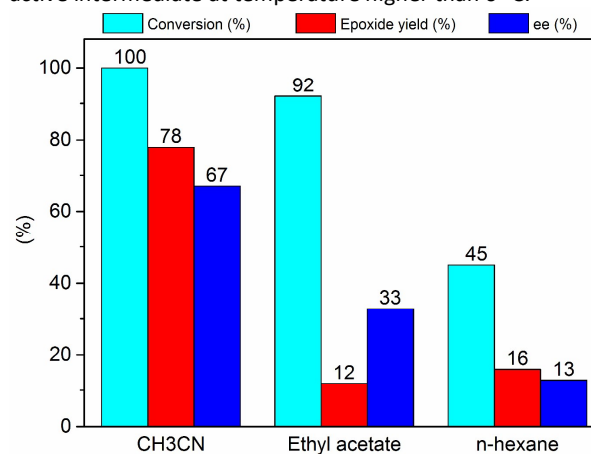

Fig. 6 Effect of solvent on the oxidation of styrene by GFC-[Mn(L)(OH)] and O$_2$. Reaction conditions: GFC-[Mn(L)(OH)] 0.010 g, styrene 2 mmol, solvent 3 ml, O$_2$ 1 bar, ^{i}PrCHO 5 mmol at 40 ºC, time 8 h. In acetonitrile the reaction time was 2 h.
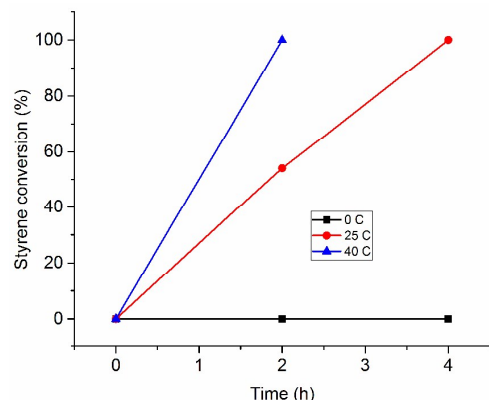
Fig. 7 Effect of the reaction temperature on the oxidation of styrene catalyzed by GFC-[Mn(L)(OH)] as a function of time. Reaction conditions: GFC-[Mn(L)(OH)] 0.01 g, styrene 2 mmol, CH$_3$CN (3 ml), O$_2$ 1 bar, ^{i}PrCHO 5 mmol.

Application scope of the catalytic system was then examined under the optimized conditions, and the results are summarized in Table 2. The results showed that in addition to the electronic nature of the olefins the steric property of the substrates influence their reactivities. Vinyl benzene derivatives (styrene, α-methyl styrene, *cis*- and *trans*-stilbene) and cyclic olefin *cis*-cyclooctene are more reactive than linear terminal olefins such as 1-decene and 1-octene. Lowest activityies (conversion 38-45%) were obtained in the oxidations of 1-octene and 1-decene (Table 2, entries 1 and 2). Epoxide selectivity and ee of α-methyl styrene and *trans*-stilbene are lower than those of styrene and *cis*-stilbene, respectively (Table 2, entries 3-6). The oxidation of *cis*-stilbene produced mainly *trans*-stilbene oxide (Table 2, entry 6). The oxidation reaction probably proceeds through a benzyl radical intermediate, which is sufficiently stable and allows free rotation about the C–C bond axis. The control experiments proved this assumption. The oxidation of styrene under optimized conditions and in the presence of hydroquinone as a radical scavenger almost stopped (conversion 5% after 8 h). This finding confirmed the radical nature of the reaction intermediate in the oxidation by GFC-[Mn(L)(OH)]/^{i}PrCHO/O$_2$ system. The catalyst was able to catalyse the oxidation of linear terminal and cyclic olefins in addition to vinyl benzene derivatives. Interestingly, the catalyst could also oxidize tetralin to 1-tetralol with 40% conversion and 28% enantioselectivity (Table 2, entry 7).

Activity, epoxide selectivity and enantioselectivity of GFC-[Mn(L)(OH)] are comparable and in some cases better than the catalytic properties of Mn/GO nanocomposite and supported Mn-salen catalysts in the oxidation of styrene with meta-chloroperbezoic acid (*m*-CPBA) and sodium hypochlorite (Table S1 in the Supplementary).[11,12,36,37] The enantioselectivity (67%) and reaction time (2 h) of GFC-[Mn(L)(OH)] are more favourable than chiral Mn(III)-salen complex of covalently grafted onto graphene oxide in the oxidation of styrene with *meta*-chloroperbezoic acid (*m*-CPBA) and sodium hypochlorite (ee 61-65% within 4-6 h).[12] The rigidity of indane-based GFC-[Mn(L)(OH)] catalyst increases the asymmetric transmission during the catalysis more than salen and
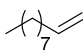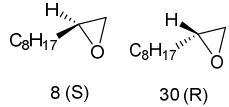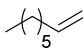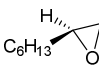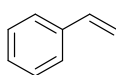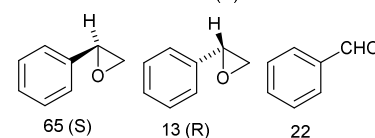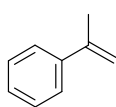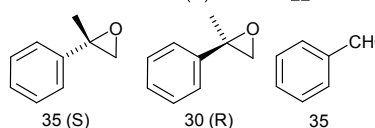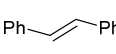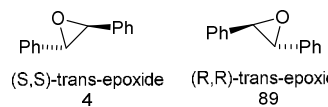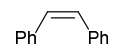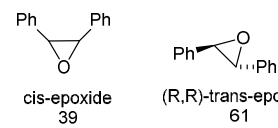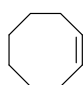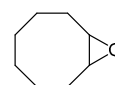
salen derivatives[38] with bulky substituents in the oxidation of styrene. Using green and clean oxidant of molecular oxygen holds promise for the future of GFC-[Mn(L)(OH)]/O$_2$/aldehyde system application.

By considering the high epoxide selectivity of catalyst (Table 2), a radical chain reaction leads to the epoxide (Scheme 2). It is predicted that the oxidation of olefins by GFC-[Mn(L)(OH)]/O$_2$/aldehyde system proceeds by the formation of acylperoxy radical by the reaction of aldehyde (isopropylaldehyde) with the Mn^{II}-complex 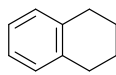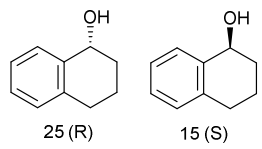which then results to the formation of acylperoxo-Mn or high valent Mn=O intermediate.[39,40] Epoxide is formed by the oxidation of olefin by the Mn^V=O.
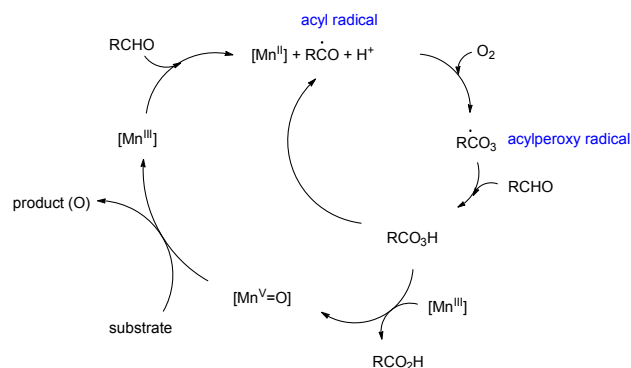
Scheme 2 Oxidation of olefins by GFC-[Mn(L)(OH)] and O$_2$/isobtyraldehyde; [Mn^{III}] represents GFC-[Mn(salan)Cl] and RCHO represents isobutyraldehyde.

Please do not adjust margins

Journal Name   **ARTICLE**

Table 2 Asymmetric oxidation of olefins with O_2 catalyzed by GFC-[Mn(L)(OH)].[a]

Entry	Substrate	Conv. (%)[b]	Product(s)/Yield (%)[b] (configuration)	Epoxide selectivity (%)	ee (%)[b] (conf.)	Time (h)
1	C_8H_{17} olefin	38	8 (S) / 30 (R) epoxides (C_8H_{17})	100	58 (R)	8
2	C_6H_{13} olefin	45	45 (S) epoxide (C_6H_{13})	100	99 (S)	8
3	styrene	100	65 (S), 13 (R) epoxide; 22 CHO	78	67 (S)	2
4	α-methylstyrene	100	35 (S), 30 (R) epoxide; 35 CHO	65	8 (S)	2
5	Ph—CH=CH—Ph	100	(S,S)-trans-epoxide 4; (R,R)-trans-epoxide 89; 7 CHO	93	92 (R,R)	8
6[c]	Ph—CH=CH—Ph (cis)	100	cis-epoxide 39; (R,R)-trans-epoxide 61	100	100 (R,R)	8
7	tetralin	40	25 (R) OH; 15 (S) OH	-	28 (R)	8
8	cyclooctene	100	cyclooctene epoxide	100	-	8

[a] Reaction conditions: catalyst GFC-[Mn(L)(OH)] 10 mg, substrate 2 mmol, O_2 1 bar, CH_3CN 3 mL, [i]PrCHO 5 mmol and temperature 40° C. [b] Conversion, selectivity and enantioselectivity were determined by GC. [c] The substrate was 0.50 mmol.

Reusability of the catalyst

The recyclability of GFC-[Mn(L)(OH)] was examined using the oxidation of styrene. The products were styrene epoxide (S-configuration and ee about 67%) and benzaldehyde. After each

ARTICLE   **Journal Name**

run, the solution was simply decanted with the assistance of an external magnet. After a simple wash with CH_3CN and the subsequent removal of residual solvent by drying at 60 °C for 6 h, the catalyst was reused for the next run. Interestingly, the obtained catalyst by immobilization of [Mn(L)(OH)] on a magnetic support (GFC) showed excellent activity and reusability for 5 recycles. The conversion was maintained at a similar level after 5 cycles (Fig. 8), however, the epoxide yield of the catalyst decreased to 65 % whereas show increasing in its enantioselectivity. Both epoxide selectivity decrease and enantioselectivity increase suggesting somewhat [Mn(L)(OH)] leaching (Table 1, entries 6 and 7). The spectra of the filtrates after each recycle are shown in Fig. S2. Slight leaching is seen after 4th recycle. The FE-SEM image of the catalyst after recycling indicated the catalyst is quite robust and no significant aggregation was found (Fig. 9)**.**

The hot filtration test was used to investigate heterogeneous nature of GFC-[Mn(L)(OH)] nanocatalyst and to make sure no leaching of Mn and/or [Mn(L)(OH)] during the course of catalytic olefin oxidation reaction. In this test, a mixture of GFC-[Mn(L)(OH)] (10 mg), styrene (2.0 mmol), [i]PrCHO (5 mmol), in CH_3CN (3 mL) was heated at 40 °C for 30 min. The GFC-[Mn(L)(OH)] catalyst was separated from the hot reaction mixture after 30 min using magnetic separation technique. Then, it was observed by using GC that 70% conversion (epoxide selectivity 74%, ee 53%) was achieved. The reaction was continued with the filtrate for 2 h at the same reaction temperature. The oxidation product conversion of 73% (epoxide selectivity 72%, ee 43%) was observed after 2 h confirmed by GC analysis. After the completion of the reaction, no detectable leaching of manganese was found by AAS analysis. The results of this study proved the stability of GFC-[Mn(L)(OH)] in the oxidation reaction condition for 2 h. The conversion of styrene in the presence of GFC-[Mn(L)(OH)] after 2 h was 100% (epoxide selectivity 78%, ee 67%) (Table 2, entry 3).
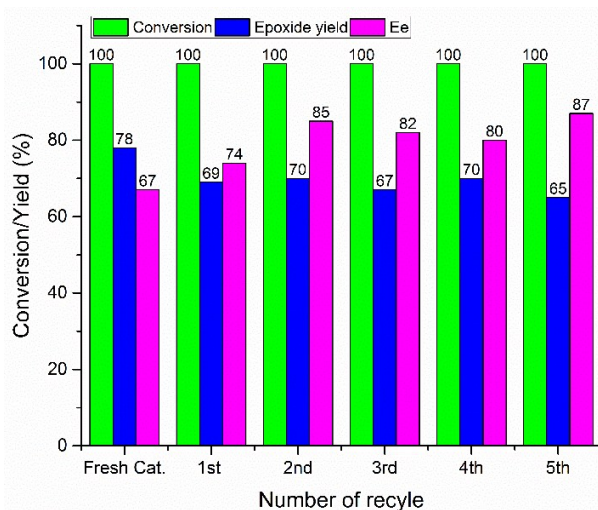

Fig. 9 FE-SEM of the recovered GFC-[Mn(L)(OH)].

The key role of GFC-[Mn(L)(OH)] catalysis is evident in the oxidation of olefins. In the absence of the catalyst no reaction occurred under our mild operating conditions with O_2/isobutyraldehyd in the oxidation of styrene (Table 1, entry 1). Probably, the oxygenation of olefins occurs by a reactive high-valent Mn-oxo intermediate which is produced by the reaction of the isopropylperoxyacid with GFC-[Mn(L)(OH)].[24] Chirality is induced by the chiral (1*R*,2*S*)-(+)-cis-1-amino-2-indanol when the olefin is closing the nanocatalyst surface.

Conclusions

In summary, we have successfully developed a new magnetically separable catalytic system by immobilization of the chiral manganese complex of (1*R*,2*S*)-(+)-cis-1-amino-2-indanol on GFC nanoparticles. The chiral GFC-[Mn(L)(OH)] showed excellent catalytic activity and enantioselectivity for the asymmetric epoxidation of various terminal, cyclic and aromatic olefins by O_2/aldehyde and could be reused at least five times. The main feature of this simple catalyst is in using almost free and green O_2 for the oxidation under mild conditions and a rigid indanol-based unit in the complex to enhance the enantioselectivity. Carbon coated magnetic Fe_3O_4 nanoparticles supported on reduced graphene oxide sheets (GFC) facilitated the separation of the catalyst, and made the GFC-[Mn(L)(OH)] catalyst reusable. Remarkable synergistic effect of reduced graphene oxide support was observed on increasing activity, epoxide selectivity and enantioselectivity. The advantages raise the prospect of using this type of simple supported catalyst for organic synthesis and epoxidation of olefins.

Acknowledgements

Fig. 8 Catalyst recyclability study for model reaction. For reaction conditions see Table 2 footnote.

Journal Name

ARTICLE

Notes and references

1. R. Davis, J. Stiller, T. Naicker, H. Jiang and K. Jorgensen, *Angew. Chem., Int. Ed. Engl.*, 2014, **53**, 7406.

2. D. Shen, B. Qiu, D. Xu, C. Miao, C. Xia and W. Sun, *Org. Lett.*, 2016, **18**, 372.

3. A. M. Zima, O. Y. Lyakin, R. V. Ottenbacher, K. P. Bryliakov, and E. P. Talsi, *ACS Catal.*, 2017, **7**, 60.

4. W. Wang, Q. Sun, D. Xu, C. Xia and W. Sun, *ChemCatChem* 2017, **9**, 420.

5. D. Shen, C. Saracini, Y.-M. Lee, W. Sun, S. Fukuzumi, and W. Nam, *J. Am. Chem. Soc.*, 2016, **138***, 15857.

6. J. Huang, X. Fu, G. Wang, Q. Miao and G. Wang, *Dalton Trans.*, 2012, **41**, 10661.

7. P. T. Anastas*, T.C. Williamson (Eds.), *Green Chemistry: Frontiers in Chemical Synthesis and Processes*, Oxford University Press, Oxford, 1998.

8. B. Zahed and H. Hosseini-Monfared, *Appl. Surf. Sci.*, 2015, **328**, 536.

9. C. Su and K. Loh, *Acc. Chem. Res.*, 2013, **46**, 2275.

10. W. Fan, W. Gao, C. Zhang, W. Tjiu, J. Pan and T. Liu, *J. Mater. Chem.*, 2012, **22**, 25108.

11. W. Zheng, R. Tan, L. Zhao, Y. Chen, C. Xiong and D. Yin, *RSC Adv.*, 2014, **4**, 11732.

12. M. Nasseri, A. Allahresani and H. Raissi, *RSC Adv.*, 2014, **4**, 26087.

13. R. Dalpozzo, *Green Chem.*, 2015, **17**, 3671.

14. G. Zhou, D. Wang, F. Li, L. Zhang, N. Li, Z. Wu, L. Wen, G. Lu and H. Cheng, *Chem. Mater.*, 2010, **22**, 5306.

15. A. Silva, V. Budarin, J. Clark, C. Freire and B. de Castro, *Carbon*, 2007, **45**, 1951.

16. J. Huang, B. Lian, Y. Qian, W. Zhou, W. Chen and G. Zheng, *Macromolecules*, 2002, **35**, 4871.

17. L. Canali, D. Sherrington and H. Deleuze, *React. Funct. Polym.*, 1999, **40**, 155.

18. R. Bikas, H. Hosseini-Monfared, T. Lis and M. Siczek, *Inorg. Chem. Commun.,* 2012, **15**, 151.

19. H. Hosseini-Monfared, R. Bikas and P. Mayer, *Inorg. Chim. Acta,* 2010, **363**, 2574.

20. O. Pouralimardan, A. –C. Chamayou, C. Janiak and H. Hosseini-Monfared, *Inorg. Chim. Acta*, 2007, **360**, 1599.

21. M. Ghorbanloo, H. Hosseini-Monfared and C. Janiak, *J. Mol. Catal. A: Chem.*, 2011, **345**, 12.

22. I. Gallou and C. Senanayake, *Chem. Rev.*, 2006, **106**, 2843.

23. L. Hadian-Dehkordi and H, Hosseini-Monfared, Green Chem., 2016, **18**, 497.

24. A. Farokhi and H. Hosseini-Monfared, *New J. Chem.*, 2016, **40**, 5032.

25. V. Abbasi, H. Hosseini-Monfared and M. Hosseini, *Appl. Organomet. Chem.*, In press, DOI: 10.1002/aoc.3554.

26. M. D. Joesten and L. J. Schaad, *Hydrogen bonding*, M. Dekker, New York, 1974.

27. K. Nakamoto, *Infrared and Raman spectra of inorganic and coordination compounds*. John Wiley & Sons, Ltd, 1986.

28. F. He, J. Fan, D. Ma, L. Zhang, C. Leung and H. Chan, *Carbon*, 2010, **48**, 3139.

29. A. Westphal, A. Klinkebiel, H. M. Berends, H. Broda, P. Kurz, and F. Tuczek, *Inorg. Chem.*, 2013, **52**, 2372.

30. A. B. P. Lever, Inorganic Electronic Spectroscopy, Elsevier, Amsterdam, 1968

31. H. Wang and Y. Hu, *Ind. Eng. Chem. Res.,* 2011, **50**, 6132.

32. S. Sadighian, H. Hosseini-Monfared, K. Rostamizadeh and M. Hamidi, *Adv Pharm Bull*, 2015, **5**, 115.

33. S. L. Wegener, T. J. Marks and P. C. Stair, *Acc. Chem. Res.*, 2012, **45**, 206.

34. J. Nakazawa, B. J. Smith and T. D. P. Stack, *J. Am. Chem. Soc.*, 2012, **134**, 2750.

35. A. Ejigu, M. Edwards and D. A. Walsh, *ACS Catal.*, 2015, **5**, 7122.

36. W. Zheng, R. Tan, S. Yin, Y. Zhang, G. Zhao, Y. Chen and D. Yin, *Catal. Sci. Technol.*, 2015, **5**, 2092.

37. I. Kuźniarska-Biernacka, C. Pereira, A. Carvalho, J. Pires and C. Freire, *Appl. Clay Sci.* 2011, **53**, 195.

38. A. Zulauf, M. Mellah, X. Hong and E. Schulz, *Dalton Trans.*, 2010, **39**, 6911.

39. Y. Yang, J. Q. Guan, P. P. Qiu and Q. B. Kan, *Transition Met. Chem*., 2010**, 35**, 263.

40. O. V. Bakhvalov, V. V. Fomenko and N. F. Salakhutdinov, *Chem. Sustainable Dev*., 2008, **16**, 633.